Electronic structure near E_F in $YBa_2Cu_3O_x$ for $6.35 \leq x \leq 6.9$: A photoemission study

Rong Liu, B. W. Veal, A. P. Paulikas, J. W. Downey, and H. Shi
Materials Science Division, Argonne National Laboratory, Argonne, Illinois 60439

C. G. Olson and C. Gu
Ames Laboratory and Department of Physics, Iowa State University, Ames, Iowa 50011

A. J. Arko and J. J. Joyce
Los Alamos National Laboratory, Los Alamos, New Mexico 87545
(Received 2 August 1991; revised manuscript received 2 December 1991)

High-resolution angle-resolved photoemission measurements are reported for $YBa_2Cu_3O_x$ when oxygen stoichiometries are in the range $6.35 \leq x \leq 6.9$. The stoichiometry dependence of spectral features at energies close to the Fermi level was monitored along major symmetry lines in the two-dimensional Brillouin zone. Along $\bar{\Gamma}$-$\bar{S}$, two bands dispersing through E_F were observed in $YBa_2Cu_3O_{6.9}$. Band calculations indicate that these are "plane"-related features. These two bands and the Fermi surfaces that they define are nearly independent of oxygen stoichiometry. The spectral weight near E_F is relatively constant for $6.4 \leq x \leq 6.9$. However, the spectral weight falls off significantly when $x = 6.35$ (insulating), although the dispersive behavior that is characteristic of the higher oxygen stoichiometries persists. This abrupt intensity change might signal the onset of an electronic structure governed by strong correlation. Along $\bar{\Gamma}$-$\bar{Y}(\bar{X})$, one band dispersing through E_F was observed in $YBa_2Cu_3O_{6.9}$. As oxygen was removed, the intensity of this dispersive feature decreased systematically. Predictions of band theory indicate that this band is a "chain"-related feature. In general, predictions of band theory appear to be quite reliable near E_F in the oxygen stoichiometry range $x \geq 6.4$, where the material shows metallic behavior.

I. INTRODUCTION

A remarkable property of the high-T_c copper oxide superconductors is that they are generally tolerant to substantial variations in electron or hole doping (by appropriate substitution or oxygen-stoichiometry variation) such that a range of behavior, from metallic to insulating, can be observed. How the electronic structure evolves as doping concentration is varied is a question of great interest.[1-7]

Angle-resolved-photoelectron-spectroscopy (ARPES) studies on $Bi_2Sr_2CaCu_2O_8$ (Refs. 8–10) and $YBa_2Cu_3O_{6.9}$ (Refs. 11–14) revealed band dispersion and, apparently, Fermi surfaces, providing support for a Fermi-liquid description of these materials. Correspondence between the photoemission measurements and predictions of band theory have generally been very good. Additional strong support for the band-theory approach has been provided by positron-annihilation measurements of the Fermi surface in $YBa_2Cu_3O_{6.9}$.[15] However, when sufficient oxygen is removed from $YBa_2Cu_3O_{6.9}$, the material becomes insulating (when oxygen stoichiometry $x < 6.4$) and the band-theory description breaks down. Band theory predicts metallic behavior even when $x = 6$.[16,17] Earlier angle-integrated photoemission studies on $YBa_2Cu_3O_x$ for $6.2 < x < 6.9$ showed a systematic decrease of the electronic density of states at the Fermi level as oxygen was depleted.[7] However, angle-resolved photoemission experiments to study the detailed behavior of the electronic structure for varied doping concentration have been lacking.

In this paper we report high-resolution ARPES studies on $YBa_2Cu_3O_x$ (Y-Ba-Cu-O) for $6.35 \leq x \leq 6.9$. The Y-Ba-Cu-O compounds with varied oxygen concentration provide a very nice system for systematic study, for their T_c's vary continuously from 92 to 0 K as the oxygen concentration x is varied from 6.9 to 6.35, as shown in Fig. 1. Furthermore, high quality single crystals with well controlled oxygen stoichiometries and sharp superconducting transitions (< 3 K) can be readily prepared.

A unique structural feature of Y-Ba-Cu-O is the presence of one-dimensional Cu-O chains. The chains appear in addition to the Cu-O planes which are common to all of the high-T_c copper oxides. It is known that oxygen vacancies appear in the chains as oxygen is removed.[18] Further, it was observed that the oxygen vacancies tend to order; apparently, a dominant ordered form is the double-cell orthorhombic (Ortho II) phase.[19-21] T_c correlates with the degree of order.[22]

Since the states near the Fermi energy are most relevant to superconductivity and other transport properties, we measured energy distribution curves (EDC's) in the vicinity of E_F (< 1 eV below E_F) with high energy resolution (< 30 meV). Measurements were made for $\mathbf{k}$ points along symmetry lines in the two-dimensional Brillouin zone (BZ) for the stoichiometries $x = 6.9$, 6.7, 6.5, 6.4, and 6.35.

We note that, for Y-Ba-Cu-O, the c axis of the unit cell is much longer than the a and b axes. Consequently, the three-dimensional BZ is very short along k_z. The typical

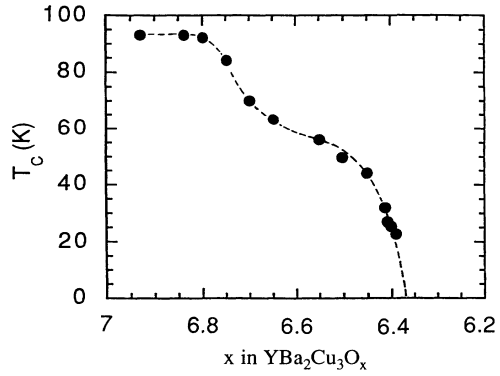

FIG. 1. Transition temperatures vs oxygen stoichiometry for $YBa_2Cu_3O_x$.

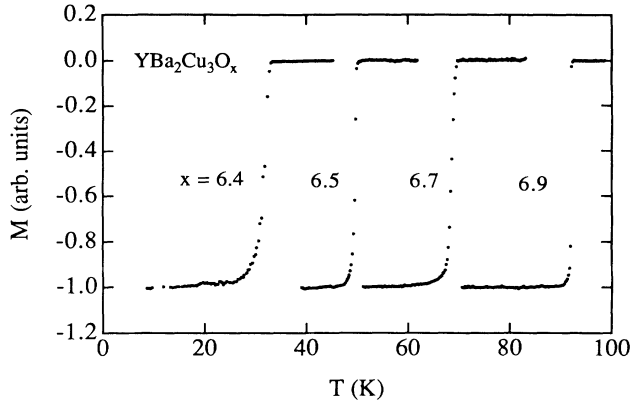

FIG. 2. Magnetization vs temperature for the measured samples of $YBa_2Cu_3O_x$. For the samples with $x=6.9$, 6.7, 6.5, and 6.4, the T_c's are, respectively, 92, 70, 50, and 33 K.

k resolution of our instruments is 0.08 $Å^{-1}$. This corresponds to about one-third of the Γ-to-Z distance, in contrast to about one-tenth of the Γ-to-X or the Γ-to-Y distance. Fortunately, for Y-Ba-Cu-O, the electronic structure is nearly two-dimensional, i.e., k_z dispersion is small. The two-dimensional nature also eliminates the problem of the indeterminacy of the momentum perpendicular to the surface in the photoemission process, thus greatly simplifying band mapping. In this paper, we make the two-dimensional approximation and use the notations $\bar{\Gamma}$, $\bar{X}$, $\bar{Y}$, and $\bar{S}$ to designate the symmetry points in the two-dimensional BZ. We note that deviations from two dimensionality may be quite substantial in some regions of the BZ.[23]

We will compare the ARPES results to the predictions of band theory.[23–25] Using the band-structure assignments, features are attributed to bands that are primarily associated with either the chains or planes. We will first discuss the features in the spectra for $x=6.9$, then present results for the lower oxygen stoichiometries, and examine systematic variations.

This paper extends the recent work of Tobin *et al.*[13] who have reported ARPES studies on single-domain (twin-free) $YBa_2Cu_3O_{6.9}$ crystals. Their data provide clear identification of chain- and plane-related features in the fully oxygenated material. ARPES studies were also reported by Campuzano *et al.*[11,12] for $YBa_2Cu_3O_{6.9}$.

II. EXPERIMENTAL DETAILS

Single crystals of Y-Ba-Cu-O with reduced oxygen stoichiometries were prepared at Argonne National Laboratory. The oxygen stoichiometries were controlled by annealing the samples at 520 °C in a flowing gas stream containing a predetermined mixture of O_2 and N_2. After equilibrating at 520 °C (60 to 160 h), the samples were quenched to liquid-nitrogen temperatures. After aging for a few days at room temperature,[22] T_c's were determined by SQUID magnetization measurements. For the SQUID measurements, samples were cooled in zero field and measured on warming (shielding). The magnetization versus temperature curves for the measured superconducting samples ($6.4 \le x \le 6.9$) are shown in Fig. 2. The transition width varies from 0.2 to 3 K. The samples with $x=6.35$ do not show a superconducting signal for temperatures above about 5 K. The resistivity in the a-b plane is shown versus temperature, in Fig. 3, when $x=6.35$. This sample shows insulating behavior (resistivity increases as temperature decreases) below about 70 K. All the measured crystals were twinned; therefore, signals from two almost orthogonal domains were simultaneously measured. In this case, $\bar{\Gamma}$-$\bar{X}$ and $\bar{\Gamma}$-$\bar{Y}$ are indistinguishable. We note that nearly all the distinct and acute spectral features observed on untwinned samples[13] were also observed on our twinned samples.

Some photoelectron spectra were acquired by using He-I radiation ($h\nu=21.2$ eV). Most of the measurements (including spectra at 21.2 eV) were made on the Ames-Montana ERG-Seya beamline[26] at the Synchrotron Radiation Center at Stoughton, Wisconsin, using mostly the Seya. For both photon sources, photoelectrons were energy analyzed by a 50-mm-radius hemispherical analyzer

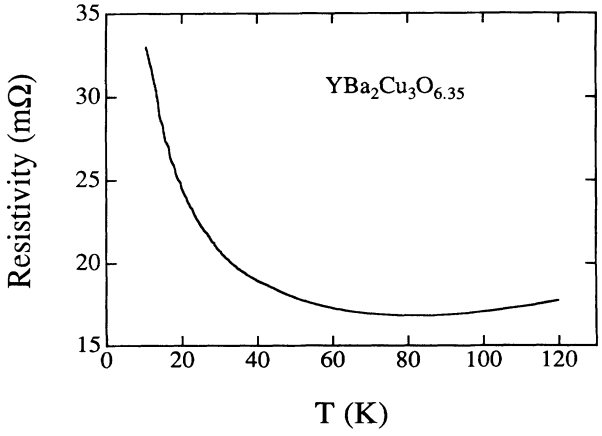

FIG. 3. The a-b resistivity vs temperature for a $x=6.35$ sample. The resistivity increases as temperature decreases below about 70 K, indicating insulator behavior.

mounted on a goniometer. The analyzer has two degrees of rotational freedom. The angular resolution of the analyzer is 2° (full apex angle of acceptance cone), which corresponds to a **k** resolution of 0.073 Å^{-1} [about $\frac{1}{11}$ of the Γ-to-$Y(X)$ distance in **k** space] for measurements near the Fermi level using 21.2 eV photons. The overall energy resolution (electron and photon) is better than 30 meV. Samples were cleaved at 20 K in a vacuum better than 4×10^{-11} Torr. The measurements were made at 20 K. Unlike the $Bi_2Sr_2CaCu_2O_8$ superconductors, where a superconducting gap was observed when the sample was cooled below T_c,[27–29] no significant difference was observed in the photoemission spectra of $YBa_2Cu_3O_{6.9}$ when data were taken above and below T_c.[13,30] The position of the Fermi level was determined by measuring the Fermi edge of a clean platinum foil which was in electrical contact with the samples.

The sample orientation was determined by Laue x-ray diffraction prior to mounting in the chamber. The cleaved surfaces contain the a-b plane. The samples were mounted with the c axis and the $a(b)$ axis in the horizontal plane. The photon beam was also in the horizontal plane striking the sample at an angle of approximately 60° from the surface normal (c axis). When synchrotron radiation was used, the photon beam was nearly completely polarized with **E** in the horizontal plane. When data were taken using He-I radiation, the surface normal was determined using a reflected laser beam from the cleaved sample surface. Otherwise, the surface normal was determined from EDC's, by monitoring the symmetry of the highly dispersive feature at about 1.5 eV binding energy that appeared with high intensity at the $\bar{\Gamma}$ point when 24 eV radiation was used. This dispersive behavior is shown in Fig. 4.

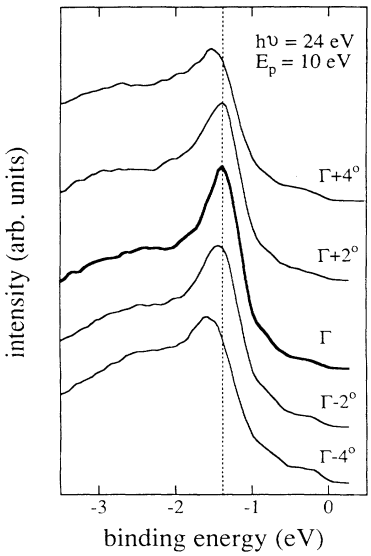

FIG. 4. EDC's for **k** points near the $\bar{\Gamma}$ point, showing the symmetry around the $\bar{\Gamma}$ point of the highly dispersive feature at about 1.5 eV binding energy.

III. RESULTS AND DISCUSSION

A. $\bar{\Gamma}$-$\bar{S}$

Shown in Fig. 5(a) are EDC's for **k** points along the $\bar{\Gamma}$-$\bar{S}$ line, for stoichiometry $x=6.9$, measured with 21.2 eV photons. The electron exit angles relative to the surface normal (θ and ϕ) are marked along each curve. Their corresponding **k** vectors, obtained from

$$\mathbf{k}_{\parallel}=0.514\ \text{Å}^{-1}\sqrt{E_{\text{kin}}(\text{eV})}\,(\sin\theta\hat{\mathbf{x}}+\sin\phi\hat{\mathbf{y}})\ ,$$

where E_{kin} is the kinetic energy, $\mathbf{k}_{\parallel}$ is the component of electron momentum parallel to the sample surface, $\hat{\mathbf{x}}$ and $\hat{\mathbf{y}}$ are the unit vectors along $\bar{\Gamma}$-$\bar{X}$ and $\bar{\Gamma}$-$\bar{Y}$ directions, respectively, are shown as open circles and solid dots in the BZ section provided with the figure. The solid lines in the BZ section (Fig. 5) show the calculated Fermi surface for stoichiometry $x=7$ of Ref. 24. (Recent highly converged calculations yield slightly different Fermi surfaces.[23,31]) We observe that, at the $\bar{\Gamma}$ point ($\theta=\phi=0°$), the spectral features are rather weak and broad. On going out toward the $\bar{S}$ point, the spectral features develop and disperse toward E_F. One prominent feature appears at about 0.25 eV below E_F at $\theta=\phi=4°$ and crosses E_F at about $\theta=\phi=9°$ (the corresponding **k** point is shown as a solid dot in the BZ). The Fermi level crossing is indicated by the abrupt decrease in the spectral intensity of a dispersing spectral peak as that peak moves toward (and through) E_F. Another feature, which appears as a shoulder at about 0.1 eV binding energy at $\theta=\phi=4°$, also disperses toward E_F and crosses the Fermi level at about $\theta=\phi=7°$. We note that these two Fermi level crossings are in close agreement with the calculated Fermi surfaces labeled (2) and (3) shown in Fig. 5.

In Fig. 6, the approximate dispersion of these two measured bands (open circles) is compared with the calculated bands of Ref. 25. As noted above, the two experimentally determined bands have approximately the same Fermi level crossings as the two calculated bands that are predicted to have dominant plane character [labeled (2) and (3) and denoted by small dots in Fig. 6]. However, the measured dispersion is smaller than predicted.

Band calculations also predict a chain band [labeled (1) and denoted by large triangular symbols in Fig. 6] that is degenerate with one of the plane bands at the Γ point, and crosses E_F at a smaller k value ($\theta=\phi\approx4°$). Because of the relatively weak intensity in the EDC's for small angles and the proximity of this band to the other two bands, it is difficult to convincingly identify this band in the spectra.

Shown in Figs. 5(b)–5(e) are EDC's for **k** points along the $\bar{\Gamma}$-$\bar{S}$ line, for stoichiometries $x=6.7$, 6.5, 6.4, and 6.35, respectively. We observe that the dispersing behavior for all these stoichiometries is remarkably similar to that of $x=6.9$. Furthermore, within the experimental uncertainty in **k** space (±1°), the bands cross E_F at about the same places in the BZ, indicating that the dimensions of the Fermi surfaces along $\bar{\Gamma}$-$\bar{S}$ are independent of oxygen stoichiometry. In fact, extensive EDC measurements

on a grid nearly covering the entire first BZ for $x=6.9$ and 6.5 show that the dimensions and the shapes of the entire Fermi surfaces are nearly the same for the two stoichiometries.[32]

Further, we observe that for stoichiometries $x=6.7$, 6.5, and 6.4, not only the band dispersions, but also the spectral line shapes and intensities are comparable to those of $x=6.9$. However, the line shape is different for $x=6.35$. We note that, for $x=6.35$, the dispersing features are less prominent and appear as shoulders, in contrast to the prominent peak structures observed at higher oxygen stoichiometries. In order to have a quantitative comparison between the spectra of different samples, we normalized the spectra to the average of the photoelectron intensity above E_F (the baseline),[5] which is mostly due to secondary electrons caused by the second-order light. (The spectra being compared were all acquired using synchrotron radiation.) Figure 7 shows overlays of the normalized spectra for $x=6.9$, 6.4, and 6.35, for the same set of **k** points along $\bar{\Gamma}$-$\bar{S}$ as shown in Fig. 5. From Fig. 7 it is clear that the spectral weight near E_F is diminished at $x=6.35$ (long dashed lines), at **k** points where bands are below E_F ($\theta,\phi<9°$). After the bands pass through E_F ($\theta,\phi>9°$), the spectra become essentially the same as those for $x=6.9$ (solid lines). For $x=6.4$ (short dashed lines), however, the spectral weight near E_F is comparable to that of $x=6.9$ at all **k** points, although the spectral features shift slightly away from E_F. Similar (perhaps slightly smaller) shifts were observed for the $x=6.5$ sample.

This shift, consistent with a sudden falloff in the density of states at the Fermi level, occurs as x approaches the metal-insulator transition. However, the shifts observed in Fig. 7 should be viewed as preliminary; more samples must be examined in the vicinity of the metal-insulator transition. It is clear, however, that a substantial change

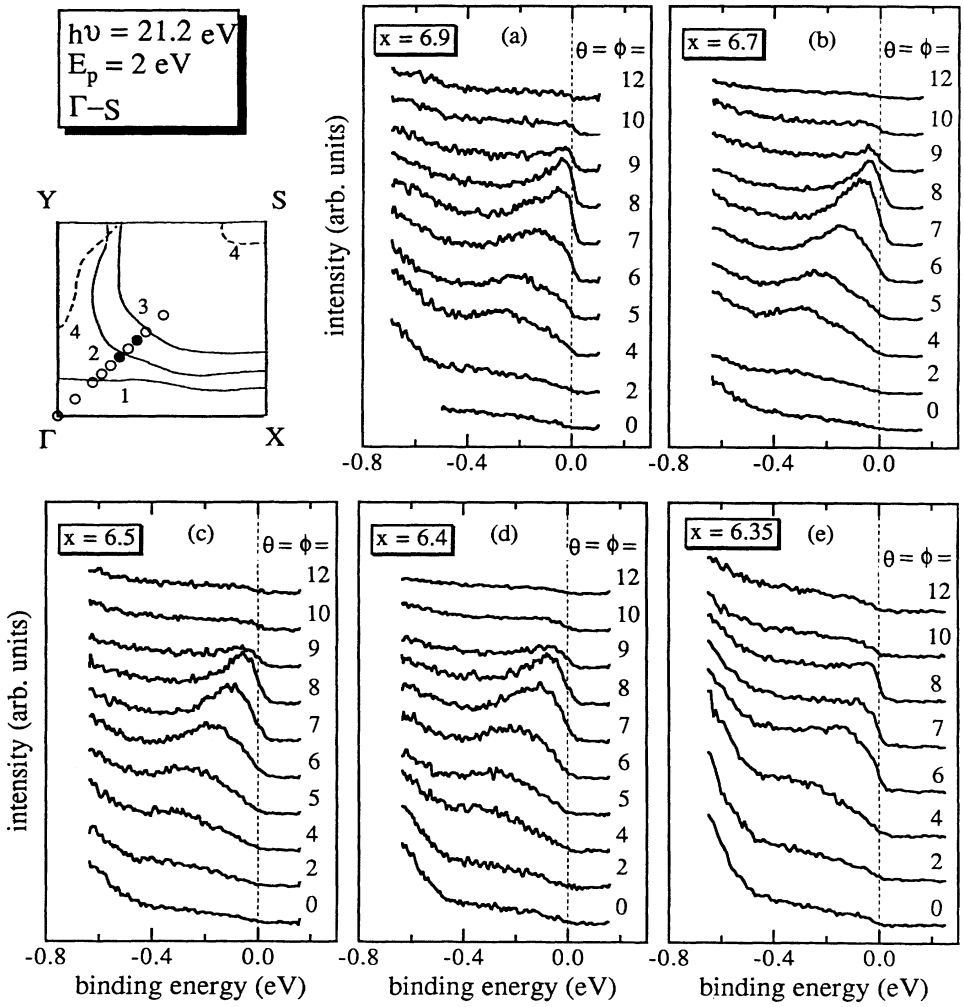

FIG. 5. EDC's for **k** points along the $\bar{\Gamma}$-$\bar{S}$ line, measured with 21.2 eV photons, for oxygen stoichiometry (a) $x=6.9$, (b) $x=6.7$, (c) $x=6.5$, (d) $x=6.4$, (e) $x=6.35$. The electron emitting angles relative to surface normal (θ and ϕ) are marked along each curve. The corresponding **k** points for the EDC's are shown as open circles and solid dots in the Brillouin zone section provided with the figure, along with the calculated Fermi surface (solid lines) of Ref. 24. The solid dots indicate experimentally determined Fermi surface crossings. The spectra for each sample have the same vertical scale, but are offset for clarity.

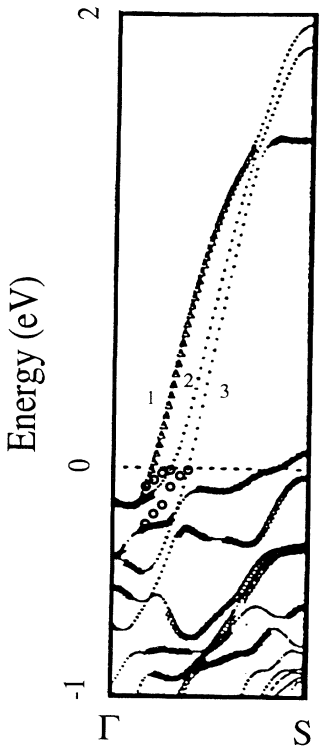

FIG. 6. Comparison of the experimentally determined band dispersion along the $\bar{\Gamma}$-$\bar{S}$ line of a $x=6.9$ sample (open circles) with the calculated bands of Ref. 25. The large triangular symbols denote bands with dominant chain character, and the small dots denote bands with dominant plane character (Ref. 25).

occurs in the spectral weight near E_F as x falls below 6.4. We note that both stoichiometries $x=6.35$ and 6.4 are very close to the metal-insulator transition (Fig. 1), but $x=6.4$ is in the superconducting regime ($T_c=33$ K) and $x=6.35$ is in the insulating regime. It appears that the abrupt falloff of the spectral weight near E_F correlates with the metal-to-insulator transition and signals a suddenly increasing role of strong correlation effects.

B. $\bar{\Gamma}$-$\bar{Y}(\bar{X})$

EDC's measured along $\bar{\Gamma}$-$\bar{Y}(\bar{X})$ show a strong dependence on photon energy,[13,30] which may be a result of k_z dispersion as indicated by band theory[23] (spectral sensitivity may vary with k_z as photon energy is changed), or strong matrix-element effects. In this paper, we shall concentrate on the results obtained with 21.2 eV photons. Other results will be discussed in separate papers.[32]

Shown in Fig. 8(a) are EDC's for **k** points along $\bar{\Gamma}$-$\bar{Y}(\bar{X})$ for stoichiometry $x=6.9$ taken with 21.2 eV photons. Again, EDC's with labeled θ values correspond to the open circles and solid dots shown in the BZ section. Because the measured samples were twinned, the **k** points are marked along both $\bar{\Gamma}$-$\bar{X}$ and $\bar{\Gamma}$-$\bar{Y}$. The most prominent feature is the spectral peak, first apparent near 0.1 eV below E_F at $\theta=7°$, and dispersing through E_F at about $\theta=15°$ (solid dot). Another feature at about 0.3 eV binding energy is also visible. It shows a small dispersion but never reaches the Fermi level. The comparison of these dispersive features with the calculated bands of Ref. 25 is shown in Fig. 9. We note that the observed band nearest E_F is in very good agreement with the calculated band along Γ-Y predicted to have mixed chain and plane character [labeled (4)]. (The detail of this band varies among calculations performed by different groups.[23–25,31]) An ARPES study of single-domain (twin-free) $YBa_2Cu_3O_{6.9}$ crystals by Tobin *et al.*[13] shows that this band is only observed along $\bar{\Gamma}$-$\bar{Y}$. This indicates that the spectral feature is dominated by chain bands since the plane bands have rather little anisotropy in the a-b plane. The observed band at higher binding energy lies nearly midway, along Γ-X, between a chain band and

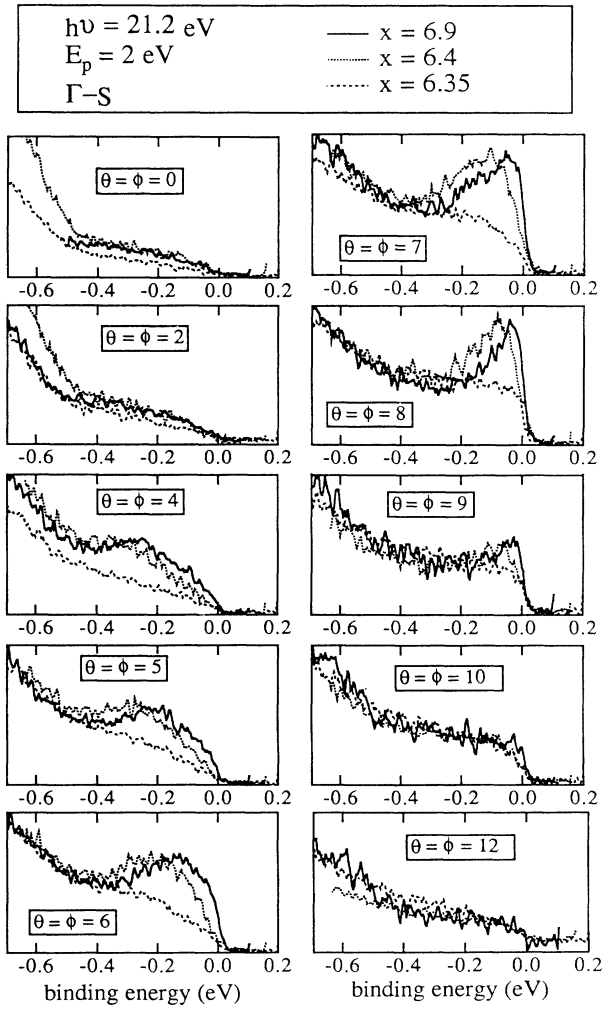

FIG. 7. EDC's for **k** points along the $\bar{\Gamma}$-$\bar{S}$ line, with the EDC's at the same **k** point for three oxygen stoichiometries, $x=6.9$, 6.4, and 6.35, superimposed. The spectra are normalized to the average of the photoelectron intensity above E_F, as described in the text. The spectral weight for $x=6.4$ is comparable to $x=6.9$, although the peak of the spectrum is slightly shifted away from the Fermi level. However, the spectral weight of the $x=6.35$ sample is diminished.

a plane band. Further studies on detwinned crystals will be needed to clarify these band assignments.

Shown in Figs. 8(b)–8(e) are the EDC's along $\bar{\Gamma}$-$\bar{Y}(\bar{X})$ for stoichiometries $x=6.7$, 6.5, 6.4, and 6.35, respectively. We observe that the sharp feature near E_F shows a systematic decrease in intensity for the entire range of oxygen stoichiometry. Such a systematic change is consistent with the assumption that the feature is associated with a band that has substantial chain character. As oxygen stoichiometry is decreased, the Cu-O chains become systematically depleted until, at $x=6$, the chains disappear. This systematic intensity variation with x contrasts with the behavior of the dispersive spectral features along $\bar{\Gamma}$-$\bar{S}$, where the intensity shows no (or very little) dependence on oxygen concentration in the metallic regime. According to band theory, the features along Γ-S are plane related and are expected to show very little dependence on oxygen stoichiometry.[16,17,33] Thus, the observed behavior, both for $\bar{\Gamma}$-$\bar{Y}(\bar{X})$ and for $\bar{\Gamma}$-$\bar{S}$, corresponds remarkably well, when oxygen stoichiometry is varied, with the predictions of band theory.

Since oxygen vacancies are introduced in abundance as x is varied, it is remarkable that the (apparently) chain-related features persist, with relatively small variation, for a wide stoichiometry range. The chain-related feature near E_F is still well defined at $x=6.7$, where the chains have acquired a large vacancy concentration; furthermore, the band remains visible through the entire metallic region of the phase diagram.

The measured band at the binding energy of about 0.2 eV does not show a strong dependence on oxygen stoichiometry. (Because of the attenuation of the peak near E_F, this higher energy peak appears even more prominently for $x=6.7$ and 6.5 than for $x=6.9$).

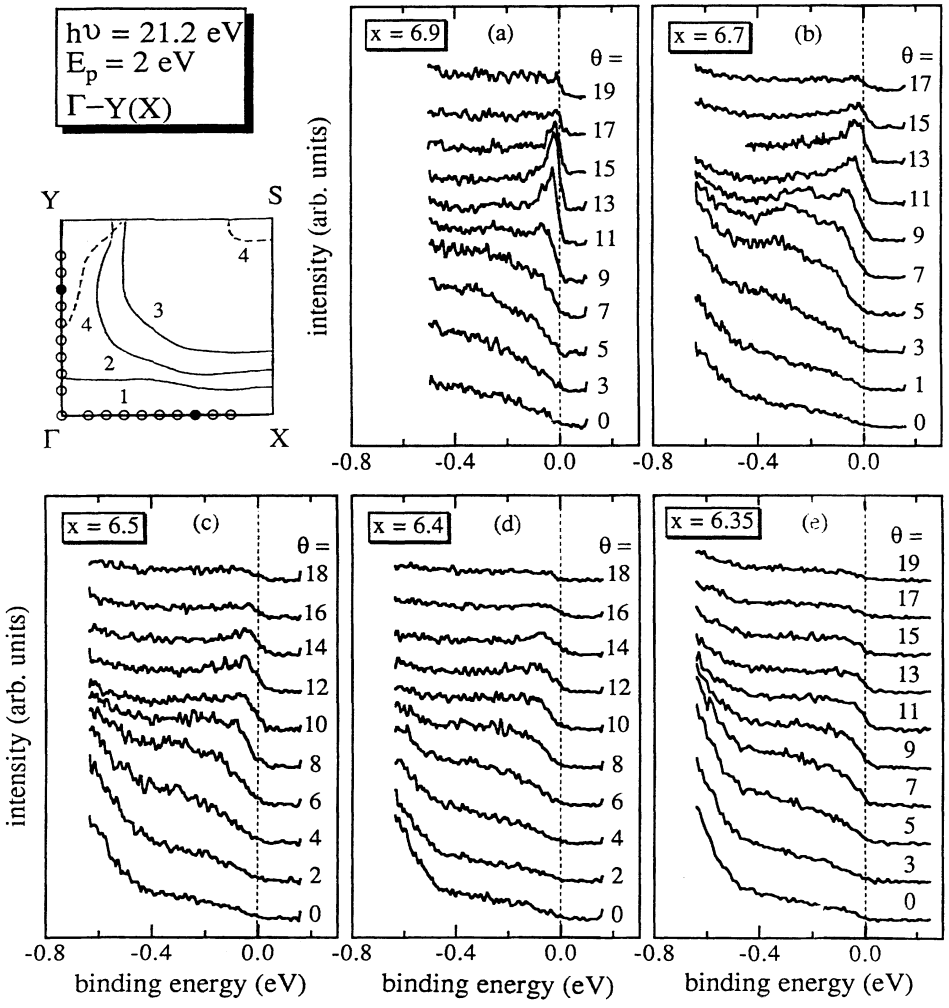

FIG. 8. EDC's for **k** points along the $\bar{\Gamma}$-$\bar{Y}(\bar{X})$ line(s), measured with 21.2 eV photons, for oxygen stoichiometry (a) $x=6.9$, (b) $x=6.7$, (c) $x=6.5$, (d) $x=6.4$, (e) $x=6.35$. The corresponding **k** points for the EDC's of (a) are shown as open circles and solid dots in the Brillouin zone section provided with the figure. Because the measured samples were twinned, **k** points are marked along both $\bar{\Gamma}$-$\bar{Y}$ and $\bar{\Gamma}$-$\bar{X}$.

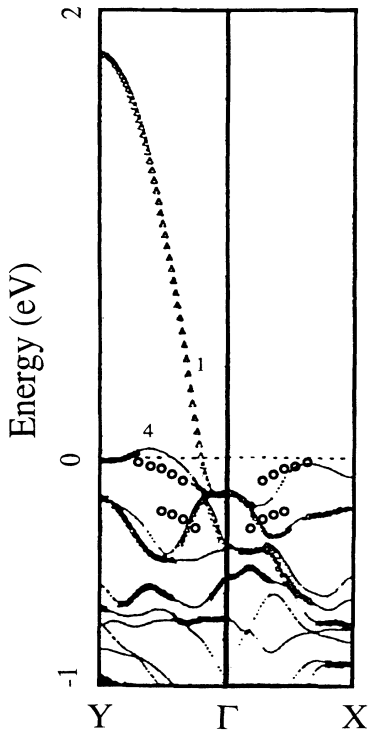

FIG. 9. Comparison of the experimentally determined band dispersion along the $\bar{\Gamma}$-$\bar{Y}(\bar{X})$ line(s) of a $x=6.9$ sample (open circles) with the calculated bands of Ref. 25. The legend is the same as in Fig. 6. Because the measured samples were twinned, the observed dispersive features are marked along both $\bar{\Gamma}$-$\bar{X}$ and $\bar{\Gamma}$-$\bar{Y}$.

C. Summary

High-resolution ARPES measurements are reported for $YBa_2Cu_3O_x$ when oxygen stoichiometries are controlled in the range $6.35 \leq x \leq 6.9$. Measurements were taken to monitor the dependence of spectral features, including variations in dispersive behavior and spectral weight, on oxygen concentration at energies close to the Fermi level. Using the predictions of band theory to guide interpretation of the data, both "chain bands" and "plane bands" were studied.

Two bands along $\bar{\Gamma}$-$\bar{S}$ dispersing through E_F were observed in $YBa_2Cu_3O_{6.9}$. Their Fermi level crossings are consistent with those of the two plane-related bands predicted by band theory, but the dispersion is smaller than predicted. These two bands and the Fermi surfaces that they define are almost independent of oxygen stoichiometry. Further, the spectral weight near E_F is relatively constant for $6.4 \leq x \leq 6.9$. However, this spectral weight falls off significantly when $x=6.35$, although the dispersive behavior, which is characteristic of the higher stoichiometries, persists. The $x=6.35$ composition is nonsuperconducting, but the stoichiometry is very close to the metal-insulator boundary. The abrupt intensity changes apparent near E_F at the metal-insulator boundary might signal the onset of strong correlation effects responsible for the insulating behavior. There is also preliminary indication that bands move away from E_F as stoichiometries approach the metal-insulator boundary.

One band, with substantial chain character, was observed in $YBa_2Cu_3O_{6.9}$ as it dispersed along $\bar{\Gamma}$-$\bar{Y}(\bar{X})$ until the band passed through the Fermi level. As oxygen was removed, the intensity of this dispersive feature systematically decreased. This behavior is unlike that observed for plane band features, which are relatively undisturbed by changes in x, and which show little intensity variation for $x \geq 6.4$. However, the systematic loss of intensity observed for the chain-related feature is consistent with the systematic destruction of chains caused by oxygen removal. In general, the behavior of ARPES data for $YBa_2Cu_3O_x$ is remarkably well described by band theory in the oxygen stoichiometry range $x \geq 6.4$, where the material shows metallic behavior.

ACKNOWLEDGMENTS

Work at Argonne National Laboratory was supported by the U.S. DOE under Contract No. W-31-109-ENG-38 (B.W.V., A.P.P., J.W.D., and H.S.) and by the NSF, Science and Technology Center for Superconductivity, under Contract No. DMR 8809854 (R.L.). Ames Laboratory was operated for the U.S. DOE by Iowa State University under Contract No. W-7405-ENG-82. Los Alamos National Laboratory was supported by the U.S. DOE. The Synchrotron Radiation Center was supported by NSF under Contract No. DMR 8601349.

[1]A. P. Kampf and J. R. Schrieffer, Phys. Rev. B **42**, 7967 (1990).
[2]A. A. Abrikosov and L. A. Falkovsky, Physica C **168**, 556 (1990).
[3]P. A. Lee, Phys. Rev. Lett. **63**, 680 (1989); N. Nagaosa and P. A. Lee, *ibid.* **64**, 2450 (1990).
[4]C. A. R. Sá de Melo and S. Doniach, Phys. Rev. B **41**, 6633 (1990).
[5]J. W. Allen, C. G. Olson, M. B. Maple, J.-S. Kang, L. Z. Liu, J.-H. Park, R. O. Anderson, W. P. Ellis, J. T. Markert, Y. Dalichaouch, and R. Liu, Phys. Rev. Lett. **64**, 595 (1990); J. W. Allen and C. G. Olson, Mater. Res. Sci. Bull. **25**, 34 (1990).
[6]T. Takahashi, H. Matsuyama, H. Katayama-Yoshida, K. Seki, K. Kamiya, and H. Inokuchi, Physica C **170**, 416 (1990).
[7]B. W. Veal, J. Z. Liu, A. P. Paulikas, K. Vandervoort, H. Claus, J. C. Campuzano, C. G. Olson, A.-B. Yang, R. Liu, C. Gu, R. S. List, A. J. Arko, and R. J. Bartlett, Physica C **158**, 276 (1989).
[8]C. G. Olson, R. Liu, D. W. Lynch, R. S. List, A. J. Arko, B. W. Veal, Y. C. Chang, P. Z. Jiang, and A. P. Paulikas, Phys. Rev. B **42**, 381 (1990); C. G. Olson, R. Liu, D. W. Lynch, B. W. Veal, Y. C. Chang, P. Z. Jiang, J. Z. Liu, A. P. Paulikas, A. J. Arko, and R. S. List, Physica C **162-164**, 1697 (1989).
[9]R. Manzke, T. Buslaps, R. Claessen, and J. Fink, Europhys.

Lett. **9**, 477 (1989); R. Manzke, T. Buslaps, R. Claessen, M. Skibowski, and J. Fink, Physica C **162-164**, 1381 (1989).

[10]B. O. Wells, Z.-X. Shen, D. S. Dessau, W. E. Spicer, C. G. Olson, D. B. Mitzi, A. Kapitulnik, R. S. List, and A. Arko, Phys. Rev. Lett. **24**, 3056 (1990).

[11]J. C. Campuzano, G. Jennings, M. Faiz, L. Beaulaigue, B. W. Veal, J. Z. Liu, A. P. Paulikas, K. Vandervoort, H. Claus, R. S. List, A. J. Arko, and R. J. Bartlett, Phys. Rev. Lett. **64**, 2308 (1990).

[12]J. C. Campuzano, G. Jennings, A. J. Arko, R. S. List, B. W. Veal, and R. Benedek, J. Phys. Chem. Solids. **52**, 1411 (1991).

[13]J. G. Tobin, C. G. Olson, C. Gu, J. Z. Liu, F. R. Solal, M. J. Fluss, R. H. Howell, J. C. O'Brien, H. B. Radousky, and P. A. Sterne, Phys. Rev. B **45**, 5563 (1992).

[14]G. Mante, R. Claessen, A. Huss, R. Manzke, M. Skibowski, Th. Wolf, M. Knupfer, and J. Fink, Phys. Rev. B **44**, 9500 (1991).

[15]L. C. Smedskjaer, J. Z. Liu, R. Benedek, D. G. Legnini, D. J. Lam, M. D. Stahulak, H. Claus, and A. Bansil, Physica C **156**, 269 (1988); H. Haghighi, J. H. Kaiser, S. Rayner, R. N. West, J. Z. Liu, R. Shelton, R. Howell, F. Solal, and M. J. Fluss, Phys. Rev. Lett. **67**, 382 (1991).

[16]Frank Herman, Robert V. Kasowski, and William Y. Hsu, Phys. Rev. B **36**, 6904 (1987).

[17]T. Fujiwara and Y. Hatsugai, Jpn. J. Appl. Phys. **26**, L716 (1987).

[18]J. D. Jorgensen, B. W. Veal, A. P. Paulikas, L. J. Nowicki, G. W. Crabtree, H. Claus, and W. K. Kwok, Phys. Rev. B **41**, 1864 (1990).

[19]J. Reyes-Gasga, T. Krekels, G. Van Tenderloo, J. Van Landuyt, S. Amelincks, W. H. M. Bruggink, and H. Verweij, Physica C **159**, 831 (1989).

[20]M. Hervieu, B. Domenges, B. Raveau, M. Post, W. R. McKinnon, and J. M. Tarascon, Mater. Lett. **8**, 73 (1989).

[21]D. deFontaine, G. Ceder, and M. Asta, J. Less-Common Met. **164 & 165**, 108 (1990); Nature **343**, 544 (1990).

[22]B. W. Veal, A. P. Paulikas, Hoydoo You, Hao Shi, Y. Fang, and J. W. Downey, Phys. Rev. B **42**, 4770 (1990); **42**, 6305 (1990); J. D. Jorgensen, S. Pei, P. Lightfoot, H. Shi, A. P. Paulikas, and B. W. Veal, Physica C **167**, 571 (1990); H. Claus, S. Yang, A. P. Paulikas, J. W. Downey, and B. W. Veal, *ibid.* **171**, 205 (1990).

[23]W. E. Pickett, R. E. Cohen, and H. Krakauer, Phys. Rev. B **42**, 8764 (1990).

[24]J. Yu, S. Massidda, A. J. Freeman, and D. D. Koelling, Phys. Lett. A **122**, 203 (1987); A. J. Freeman, J. Yu, S. Massidda, and D. D. Koelling, Physica C **148B**, 212 (1987).

[25]H. Krakauer, W. E. Pickett, and R. E. Cohen, J. Supercond. **1**, 111 (1988); W. E. Pickett, Rev. Mod. Phys. **61**, 433 (1989).

[26]C. G. Olson, Nucl. Instrum. Methods A **266**, 205 (1988).

[27]J. M. Imer, F. Pathey, B. Dardel, W. D. Schneider, Y. Baer, Y. Petroff, and A. Zettl, Phys. Rev. Lett. **62**, 336 (1989).

[28]C. G. Olson, R. Liu, A. B. Yang, D. W. Lynch, R. S. List, A. J. Arko, B. W. Veal, Y. C. Chang, P. Z. Jiang, and A. P. Paulikas, Science **245**, 731 (1989); Solid State Commun. **76**, 411 (1990).

[29]R. Manzke, T. Buslaps, R. Claessen, and J. Fink, Europhys. Lett. **9**, 477 (1989).

[30]R. Liu, B. W. Veal, A. P. Paulikas, J. W. Downey, H. Shi, C. G. Olson, C. Gu, A. J. Arko, J. J. Joyce, and R. J. Bartlett, J. Phys. Chem. Solids **52**, 1437 (1991).

[31]J. Yu *et al.* (unpublished).

[32]R. Liu *et al.* (unpublished).

[33]J. Yu *et al.* (unpublished).